Supplementary Material to:
Evaluation of MARv3.14 over the Greenland Ice Sheet

Guillaume Timmermans, Brice Noël, Christoph Kittel, Thomas Dethinne, Nicolas Ghilain and Xavier Fettweis

Correspondence to: gtimmermans@uliege.be

Table S1. MAR version 3.14 (at 5 and 15 km resolution) SMB evaluation in the exact same way as the latest SMB model intercomparison from Fettweis et al. (2020) and comparison to the result of MAR version 3.9 at 15 km resolution (the version used for the intercomparison). All numbers except correlations are in m w.e.. For each dataset, we provide the number of observations (no.), the mean and the standard deviation. Fettweis et al. (2020) used MAR at 15 km resolution.

	Ice cores			Air-bone radar		
	no. 260 ; 0.33 ± 0.08 m w.e.			no. 9043 ; 0.17 ± 0.13 m w.e.		
	Bias	RMSE	Correlation	Bias	RMSE	Correlation
MARv3.9 15 km	0.01	0.08	0.93	-0.01	0.02	0.99
MARv3.14 15 km	-0.01	0.07	0.92	-0.01	0.02	0.98
MARv3.14 5 km	0.01	0.07	0.92	-0.01	0.02	0.99
	Snow pits			PROMICE – main ice sheet		
	no. 130 ; 0.41 ± 0.34 m w.e.			no. 1438 ; -0.92 ± 0.62 m w.e.		
	Bias	RMSE	Correlation	Bias	RMSE	Correlation
MARv3.9 15 km	-0.08	0.37	0.68	0.10	0.48	0.93
MARv3.14 15 km	-0.01	0.32	0.80	0.12	0.46	0.94
MARv3.14 5 km	-0.01	0.32	0.81	0.04	0.44	0.94

Table S2. Statistics (bias, RMSE, R^2, and correlation) for the comparison between MAR-simulated and observed SMB (using data from SUMup Vandecrux et al. (2024) and Ohmura and Reeh (1991)). "Raw" refers to results obtained using IDW interpolation (Eq. A1). The second part "Corrected" reports the statistics after applying the elevation correction (Eq. 1).

Resolution	**Bias** [m w.e.]	**RMSE** [m w.e.]	**R^2**	**Correlation**
		Raw		
5 km	0.111	0.505	0.847	0.93
10 km	0.221	0.702	0.706	0.87
15 km	0.287	0.825	0.592	0.82
20 km	0.285	0.843	0.575	0.80
30 km	0.356	0.984	0.421	0.72
		Corrected		
5 km	0.079	0.407	0.901	0.95
10 km	0.103	0.442	0.883	0.94
15 km	0.114	0.480	0.862	0.93
20 km	0.118	0.492	0.855	0.93
30 km	0.173	0.604	0.782	0.90

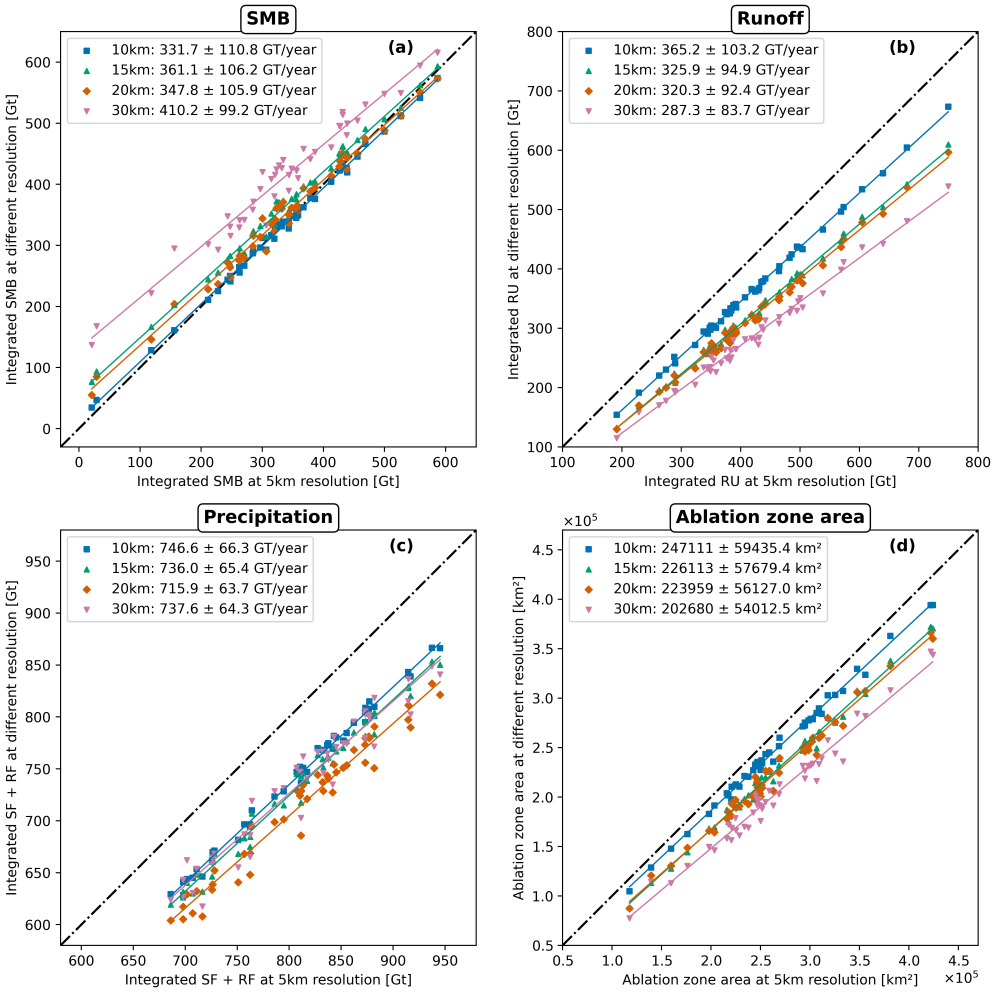

Figure S1. Comparison of (a) integrated SMB, (b) runoff, (c) precipitation, and (d) ablation zone area at different resolutions relative to the 5 km-resolution simulation, using each simulation's native grid (NG). Each point corresponds to one year, and coloured curves represent linear regressions. Values in the legend correspond to the 1979–2024 mean SMB, RU, PR or ablation zone area and and standard deviation (after the ± sign). Black dash-dotted lines indicate the 1:1 reference line.

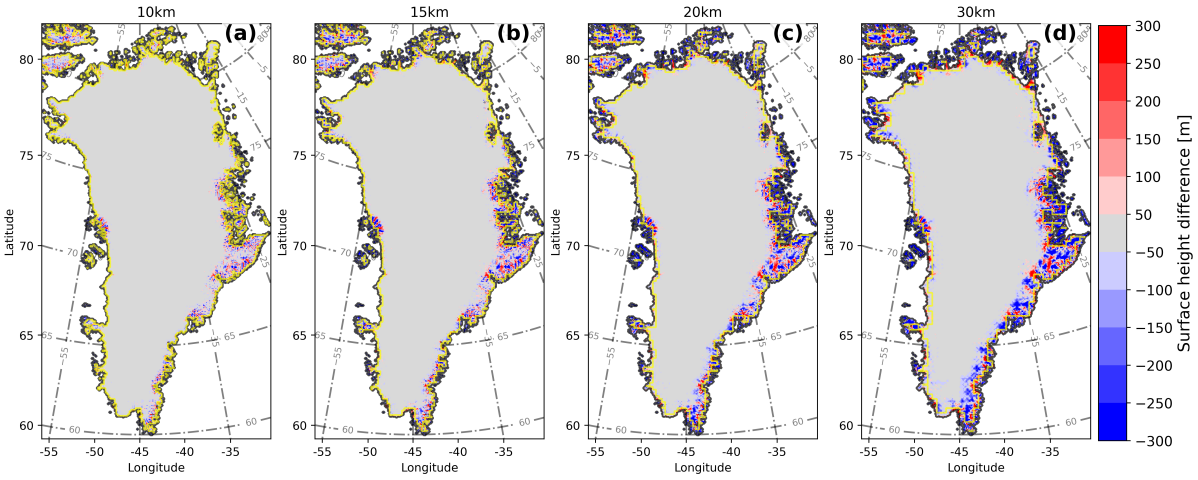

Figure S2. Differences in surface height between MAR at (a) 10 km, (b) 15 km, (c) 20 km, and (d) 30 km and MAR at 5 km. Surface height at 10–30 km were IDW-interpolated on the 5 km MAR grid. Yellow lines delineate the contour of the ice sheet mask.

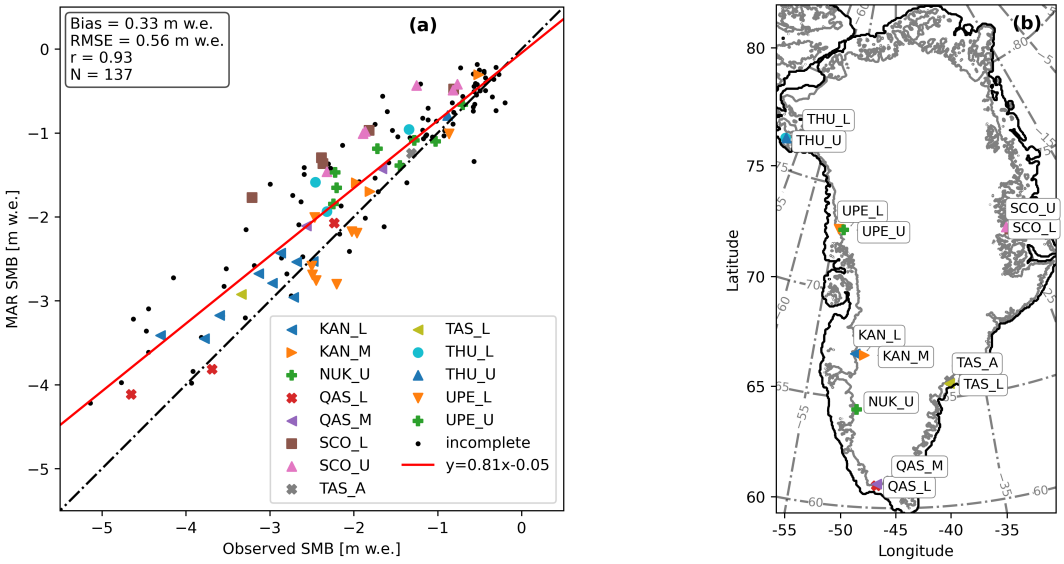

Figure S3. (a) Scatter plot of MAR SMB versus PROMICE AWS SMB (retrieved from the SUMup database) measured during summer (JJA) using pressure transducers. The 1:1 line is shown in black and the linear regression line in red. The text box indicates the mean bias, RMSE, correlation coefficient (r), and number of observations (N). Points discussed in the text (Table 2), i.e., those with sufficiently long measurement periods (>30 days) and uninterrupted measurements of the associated variables listed in Table 2, are shown with a station-specific colour and marker. Black dots correspond to measurements with shorter record lengths (10–30 days) or missing associated variables and are excluded from the main analysis. (b) Location of the PROMICE stations that appears in Table 2 on a map of Greenland. Black lines delineate continental coastlines and gray lines delineate the ice sheet and glaciers.

Table S3. Evaluation of MAR near surface meteorology at different resolutions (comparing it to automatic weather stations from PROMICE and GC-NET (Fausto et al., 2021; How et al., 2022; Vandecrux et al., 2023). The units of RMSEs and biases are indicated for each variable.

Resolution	**RMSE**	**Bias**	**Correlation**	**RMSE**	**Bias**	**Correlation**
		All year			**JJA**	
			2-meters Temperature [°C]			
5 km	2.49	0.21	0.98	1.83	-0.26	0.93
10 km	2.65	-0.56	0.97	1.93	-0.52	0.93
15 km	3.01	-0.82	0.97	2.19	-0.54	0.91
20 km	3.13	-0.71	0.96	2.33	-0.23	0.90
30 km	3.51	-0.99	0.95	2.49	-0.43	0.88
			Specific humidity [$\mathrm{g\,kg^{-1}}$]			
5 km	0.36	0.05	0.97	0.47	0.15	0.91
10 km	0.34	-0.01	0.97	0.44	0.09	0.91
15 km	0.36	-0.01	0.97	0.46	0.09	0.91
20 km	0.37	-0.02	0.96	0.48	0.07	0.90
30 km	0.39	-0.01	0.96	0.49	0.09	0.89
			Wind speed [$\mathrm{m\,s^{-1}}$]			
5 km	1.98	-0.13	0.78	1.59	-0.50	0.79
10 km	2.40	1.15	0.76	1.76	0.57	0.75
15 km	2.03	-0.13	0.76	1.64	-0.49	0.77
20 km	2.45	1.14	0.74	1.76	0.48	0.73
30 km	2.38	-0.58	0.69	2.02	-0.93	0.69
			Surface pressure [hPa]			
5 km	15.41	-3.10	0.99	15.42	-3.24	0.99
10 km	22.31	-5.52	0.97	21.73	-5.56	0.97
15 km	23.70	-5.07	0.97	22.96	-4.99	0.97
20 km	22.92	-3.54	0.97	22.19	-3.62	0.97
30 km	29.78	-7.28	0.95	28.87	-7.10	0.95

Table S4. Evaluation of MAR SEB radiative fluxes at different resolutions (compared to automatic weather stations from PROMICE and GC-NET (How et al., 2022; Fausto et al., 2021; Vandecrux et al., 2023).

Resolution	**RMSE** [$\mathrm{W\,m^{-2}}$]	**Bias** [$\mathrm{W\,m^{-2}}$]	**Correlation**	**RMSE** [$\mathrm{W\,m^{-2}}$]	**Bias** [$\mathrm{W\,m^{-2}}$]	**Correlation**
	All year			**JJA**		
Downward shortwave radiation (SWD)						
5 km	35.18	-1.33	0.96	48.92	-2.06	0.86
10 km	35.22	1.34	0.96	49.07	4.93	0.86
15 km	35.27	1.80	0.96	49.25	5.97	0.86
20 km	35.84	2.22	0.96	50.40	7.35	0.85
30 km	36.45	1.83	0.96	51.65	6.92	0.84
Downward longwave radiation (LWD)						
5 km	25.43	-9.78	0.89	22.28	-9.27	0.84
10 km	27.59	-14.20	0.89	25.39	-14.43	0.83
15 km	28.02	-14.83	0.89	25.99	-15.03	0.83
20 km	28.64	-15.12	0.88	26.95	-15.90	0.82
30 km	29.02	-14.31	0.87	27.73	-15.72	0.80
Upward shortwave radiation (SWU)						
5 km	30.90	-1.78	0.95	42.12	-0.19	0.89
10 km	31.83	0.07	0.95	45.83	5.77	0.87
15 km	33.16	0.70	0.94	48.08	7.49	0.86
20 km	35.34	4.16	0.94	51.70	14.93	0.84
30 km	36.34	1.44	0.93	53.41	8.83	0.82
Upward longwave radiation (LWU)						
5 km	10.98	-0.65	0.96	7.45	-1.20	0.93
10 km	12.12	-3.15	0.95	8.72	-2.75	0.91
15 km	13.06	-4.08	0.95	9.35	-3.02	0.90
20 km	12.95	-3.50	0.95	9.85	-2.93	0.89
30 km	14.14	-4.15	0.94	10.17	-1.93	0.87

Table S5. Comparison between MAR and PROMICE (excluding GC–NET) AWSs for the shortwave (SWD) and longwave (LWD) downwards radiative fluxes. We list results of MAR version 3.9 (15km resolution) and version 3.14 (15 and 5km resolution). We use the exact same comparison method as Delhasse et al. (2020): i.e., our comparison spans the 2010–2016 period, using an IDW interpolation without topography correction. We exclude outliers stations (SCO_L, QAS_U, NUK_U, TAS_U for both fluxes, and NUK_L only for SWD) following Delhasse et al. (2020). All statistics except correlations are in $\mathrm{W\,m^{-2}}$. Delhasse et al. (2020) used MAR at 15km resolution.

Model	**Annual**				**JJA**			
	Bias	RMSE	RMSEc	Correlation	Bias	RMSE	RMSEc	Correlation
	LWD [$\mathrm{W\,m^{-2}}$]							
MARv3.9 15 km	-10.58	26.20	23.54	0.87	-15.12	24.33	18.61	0.79
MARv3.14 15 km	-13.16	24.85	20.90	0.89	-13.56	21.64	16.64	0.83
MARv3.14 5 km	-9.13	23.43	21.09	0.89	-8.51	19.51	17.19	0.81
	SWD [$\mathrm{W\,m^{-2}}$]							
MARv3.9 15 km	-7.95	32.8	31.3	0.97	-4.42	46.07	44.41	0.88
MARv3.14 15 km	-3.8	30.75	30.04	0.97	-0.22	43.14	42.17	0.89
MARv3.14 5 km	-7.4	31.88	30.81	0.97	-10.47	45.46	43.9	0.88

Table S6. Evaluation of MAR albedo at different resolutions against OLCI–GEUS albedo (Vandecrux et al., 2021). Statistics were computed by averaging OLCI–GEUS albedo onto the MAR grids at each resolution for 2017–2019, using (1) May–September data and (2) June–July–August (JJA) data.

Resolution	**RMSE**	**Bias**	**Correlation**	**R^2**	**RMSE**	**Bias**	**Correlation**	**R^2**
	May–September				**JJA**			
5 km	0.083	-0.0017	0.689	-0.347	0.078	0.0001	0.746	0.095
10 km	0.085	0.0012	0.676	-0.409	0.080	0.0035	0.737	0.055
15 km	0.084	0.0014	0.664	-0.485	0.081	0.0042	0.724	-0.004
20 km	0.084	0.0011	0.658	-0.463	0.081	0.0039	0.717	0.010
30 km	0.084	0.0012	0.635	-0.657	0.081	0.0043	0.692	-0.123

Table S7. Evaluation of MAR $\mathrm{SWD_{abs}}$ and albedo (α) at different resolutions (compared to automatic weather stations from PROMICE and GC-NET (How et al., 2022; Fausto et al., 2021; Vandecrux et al., 2023).

Resolution	**RMSE**	**Bias**	**Correlation**	**RMSE**	**Bias**	**Correlation**
	All year			**JJA**		
Absorbed downward shortwave radiation ($\mathrm{SWD_{abs}}$) [$\mathrm{W\,m^{-2}}$]						
5 km	33.69	-7.76	0.81	37.64	-9.82	0.80
10 km	35.27	-8.37	0.79	40.06	-10.74	0.77
15 km	35.93	-8.89	0.78	41.03	-11.79	0.77
20 km	35.56	-7.88	0.78	40.37	-10.06	0.77
30 km	38.19	-10.24	0.76	43.78	-13.20	0.73
Albedo (α) [–]						
5 km	0.14	0.03	0.79	0.13	0.04	0.85
10 km	0.15	0.04	0.74	0.15	0.05	0.79
15 km	0.15	0.04	0.74	0.15	0.06	0.78
20 km	0.15	0.04	0.73	0.15	0.05	0.78
30 km	0.17	0.05	0.67	0.17	0.06	0.72

Table S8. RMSE, bias and correlation for the comparison between MAR and AMSR-derived data (Picard, 2025) for varying melt thresholds. We compare MAR to the combination of ascending and descending data (if one pass is detecting melt, then we consider the whole pixel as melting for the day).

Melt threshold [$\mathrm{mm\,w.e.\,day^{-1}}$]	**RMSE** [$\mathrm{km^2\,day^{-1}}$]	**Bias** [$\mathrm{km^2\,day^{-1}}$]	**Correlation**
0.1	37,405	6,438	0.95
0.2	36,717	1,801	0.95
0.3	37,005	-721	0.94

Table S9. RMSE, bias and correlation for the comparison between MAR and AMSR-derived data (Picard, 2025). We use a melt-based criterion of 0.2 $\mathrm{mm\,w.e.\,day^{-1}}$. We compare MAR to the combination of ascending and descending data (if one pass is one, then we consider the whole pixel as melting)

Resolution	**RMSE** [$\mathrm{km^2\,day^{-1}}$]	**Bias** [$\mathrm{km^2\,day^{-1}}$]	**Correlation**
5 km	36,717	1,801	0.95
10 km	38,978	-1,886	0.95
15 km	39,001	-2,997	0.95
20 km	40,030	-2,322	0.94
30 km	42,290	3,659	0.94